Editors' Suggestion

Abyss Aerosols: Drop Production from Underwater Bubble Collisions

Xinghua Jiang,[1] Lucas Rotily,[2] Emmanuel Villermaux,[2,3,*] and Xiaofei Wang[1,4,5,†]

[1]Department of Environmental Science and Engineering, Shanghai Key Laboratory of Atmospheric Particle Pollution and Prevention, Fudan University, Shanghai 200433, China

[2]Aix Marseille Université, CNRS, Centrale Marseille, IRPHE UMR 7342, 13384 Marseille, France

[3]Institut Universitaire de France, 75005 Paris, France

[4]Shanghai Institute of Pollution Control and Ecological Security, Shanghai 200092, China

[5]Fudan Zhangjiang Institute, Shanghai 201203, China

(Received 20 February 2024; accepted 22 May 2024; published 8 July 2024)

Over the past century, drops production mechanisms from bubble bursting have been extensively studied. They include the centrifugal fragmentation of liquid ligaments from the bubble cap during film rupture, the flapping of the cap film, and the disintegration of Worthington jets after cavity collapse. We show here that a dominant fraction of previously identified as "surface bubble bursting" submicron drops are, in fact, generated underwater, in the abyss, inside the bubbles themselves before they have reached the surface. Several experimental evidences demonstrate that these drops originate from the flapping instability of the film squeezed between underwater colliding bubbles. This finding, emphasizing the eminent role of bubble-bubble collisions, alters fundamentally our understanding of fine aerosol production and opens a novel perspective for transfers across water-air interfaces.

DOI: 10.1103/PhysRevLett.133.024001

Submicron drops, especially those originating from bursting bubbles at the ocean surface, constitute the primary natural source of atmospheric aerosols on Earth [1–4]. These drops are crucial in mass and momentum transfer processes [5–7], prevalent in both natural and industrial settings, and significantly impact the environment, human health, and climate [8–10]. Their role in affecting climate and concentrating organic pollutants and pathogens in aquatic environments has led to extensive research concerning their production mechanisms over the last century [11–13]. They are usually classified according to two major pathways: film drops produced by the rupture of the bubble cap film [5,14,15] and jet drops produced by the disintegration of Worthington jets after cavity collapse following the bubble cap rupture [16–18]. A considerable proportion of these drops are smaller than 1 μm [12]. Bursting of sub-100 μm bubbles do produce submicron jet drops [18], while it has recently been shown that the cap flapping instability of submillimeter bubbles produces submicron film drops [15]. Detailed studies, however, all concern mechanisms occurring *after* bubbles have reached the liquid surface [5,19,20]. The present study reports, by contrast, a novel and significant phenomenon: underwater collisions of bubbles produce a substantial amount of submicron drops *within* the bubbles themselves, *before* they have reached the surface, burst, and finally release these fine aerosols in air.

We start with an intriguing experimental observation: we introduce a particle-free airflow through a needle or a porous glass filter in a water solution (3.5% sodium chloride) to produce bubbles of a specific size (see Supplemental Material [21]). If all the drops would solely originate from bubble bursting at the liquid surface, then the number of submicron drops produced per bubble, the yield denoted $n(R)$, would primarily depend on the surface bubble cap curvature radius R. Altering the airflow rate should not affect $n(R)$ as long as the bubble size remains constant [4,5,17]. Indeed, at lower airflow rates, for bubbles with a size $R \sim 1700$ μm (see additional results for bubble R in the range of $600 < R < 3000$ μm in Supplemental Material [21]), $n(R)$ remains insensitive to the airflow rate [Fig. 1(a)]. However, upon reaching a certain airflow threshold, ∼6–10 ml/min, $n(R)$ jumps by up to 2 orders of magnitude when the airflow rate is further increased. This dramatic increase and the existence of an airflow threshold cannot be accounted for by standard surface bubble bursting.

One might wonder if collective effects, like multiple bubbles coalescing in a raft at the liquid surface before bursting [31,32], could explain this sharp transition of $n(R)$: the production rates of bubbles in our experiments (∼5–30 no./s) are, however, an order of magnitude below the minimum rate (∼500 no./s) reported in [31] for the onset of a collective anomaly. Also, in pure water with NaCl, surface bubbles have a lifetime ranging from approximately 0.1 to 1 s [31,33] which prevents extensive formation of bubble clusters on the surface. In addition, the total drop production rate would not be significantly altered by bubble coalescence. For example, consider ten bubbles with $R \approx 2000$ μm at the water surface. If they burst

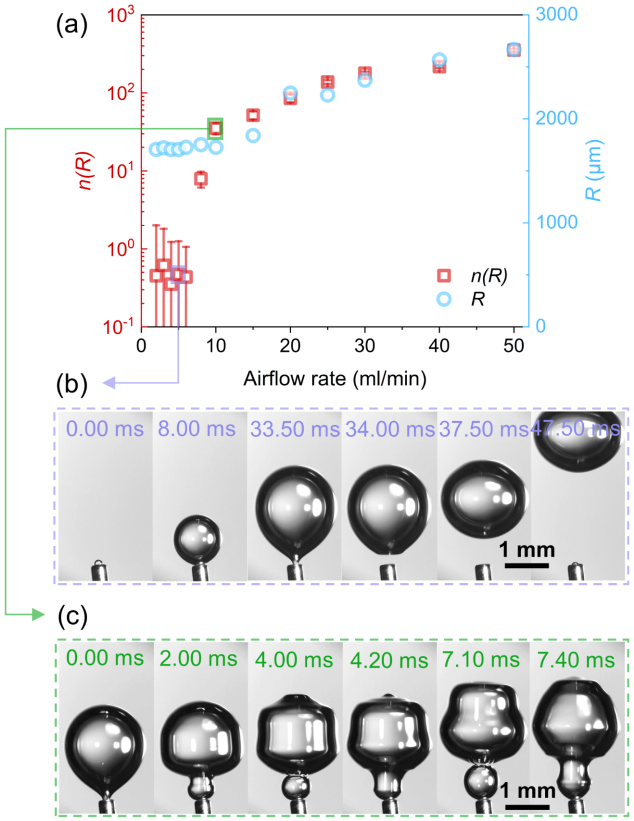

FIG. 1. Relation between submicron drop production rate and airflow rate used to produce bubbles through a needle. (a) Number of submicron drops produced per bubble $n(R)$, from a range of airflow rates and corresponding bubble size R (see details in Supplemental Material [21]). Red hollow squares represent $n(R)$ for different flow rates, corresponding to the red left axis. Blue hollow circles depict the average R of bubbles, corresponding to the blue right axis. A ~ 0.21 mm inner diameter needle producing $R \sim 1700$ μm bubbles in water with an airflow rate of (b) 5 and (c) 10 ml/min, respectively, illustrating the difference in bubble formation below and above the threshold airflow rate (see videos in Supplemental Material [21]).

individually, a total of approximately 20 submicron drops is produced [15]. Now, assume coalescence between 2, 5, or the 10 bubbles. Owing to volume conservation, coalescences would result in the formation of 5 bubbles with $R \approx 2450$ μm, 2 bubbles with $R \approx 3200$ μm, or 1 bubble with $R \approx 4000$ μm, respectively. The total number of submicron drops produced would thus be 17, 14, or 12, respectively [15]. Hence, bubble coalescence would not increase $n(R)$ but would, in fact, decrease it.

Pursuing our observations, we note that changing the airflow rate through the feeding needle influences the bubble formation process itself. Below the threshold, each bubble forms individually, with no interaction with the ones preceding and following it [Fig. 1(b)]. Increasing the airflow rate causes the bubble emission frequency to increase and, at some point, bubbles formed earlier collide with those formed subsequently [Fig. 1(c)]. Therefore, the most significant change at the threshold airflow rate is the initiation of bubble-bubble collisions, which significantly affect $n(R)$.

Based on the above observations, a natural hypothesis arises: underwater bubble-bubble collisions produce submicron drops inside the bubbles that release them in the atmosphere as their cap bursts once they have reached the surface; these drops have up to now been mistakenly attributed to bubbles bursting at the surface [3,5], but are, in fact, formed earlier in the bubble's life (see also the Sect. S5 in the Supplemental Material [21]). To test this hypothesis, we need to answer two specific questions: (I) Do these drops primarily originate from underwater bubble collisions? (II) If so, what is their production mechanism?

To address question (I), we conduct an experiment comparing the outcome of the drops in conditions with and without colliding bubbles [Fig. 2(a)]. Two bubble streams are produced from two needles at a distance apart, which can be varied. In one setting, the distance is approximately equal to three bubble diameters so that the bubbles from each needle are independent ["no collision" group in Fig. 2(b)], while in the other setting the distance is one bubble diameter to enforce collisions between bubbles emitted by one needle and the other ["collision" group in Fig. 2(c)]. The drops produced are transported to the measuring system by particle-free carrier air at a flow rate of 1 L/min and are dried through a silica diffusion dryer. The concentrations and size distributions of dried drops are quantified using a condensational particle counter and a scanning mobility particle sizer, respectively (see details in Supplemental Material [21]). To target submicron-size drops, an impactor is placed before the measurement system to remove most supermicron drops. Figure 2(d) shows that the $n(R)$ for the collision group is at least 1 order of magnitude larger than for the no collision group, clearly demonstrating that bubble-bubble collisions dramatically favor the production of submicron drops. Not only their number, but also the drops sizes distribution is different upon collision: compared to the shallower distribution in the no collision group, the collision group exhibits a distinct peak [Fig. 2(e)], indicative of the onset of a new mechanism in that case [the sources bubbles sizes distributions are close to identical for both groups, as seen in Fig. 2(f)].

We now consider question (II), namely, the mechanistic interpretations of these observations. Although this does not involve collisions *per se*, it is known that fast jets may be shot within a bubble detaching from a needle [34–37]. These jets can collide with the bubble inner wall to produce submicron splash drops, provided the collision is strong enough: splashing occurs for impact Weber numbers $\mathrm{We} = \rho v_j r/\sigma \gtrsim 100$ if v_j denotes the jet velocity, r its radius, σ the liquid surface tension, and ρ its density [38]. The phenomenon does occur in our experiments, at flow rates below the threshold [21]. The corresponding jet diameter

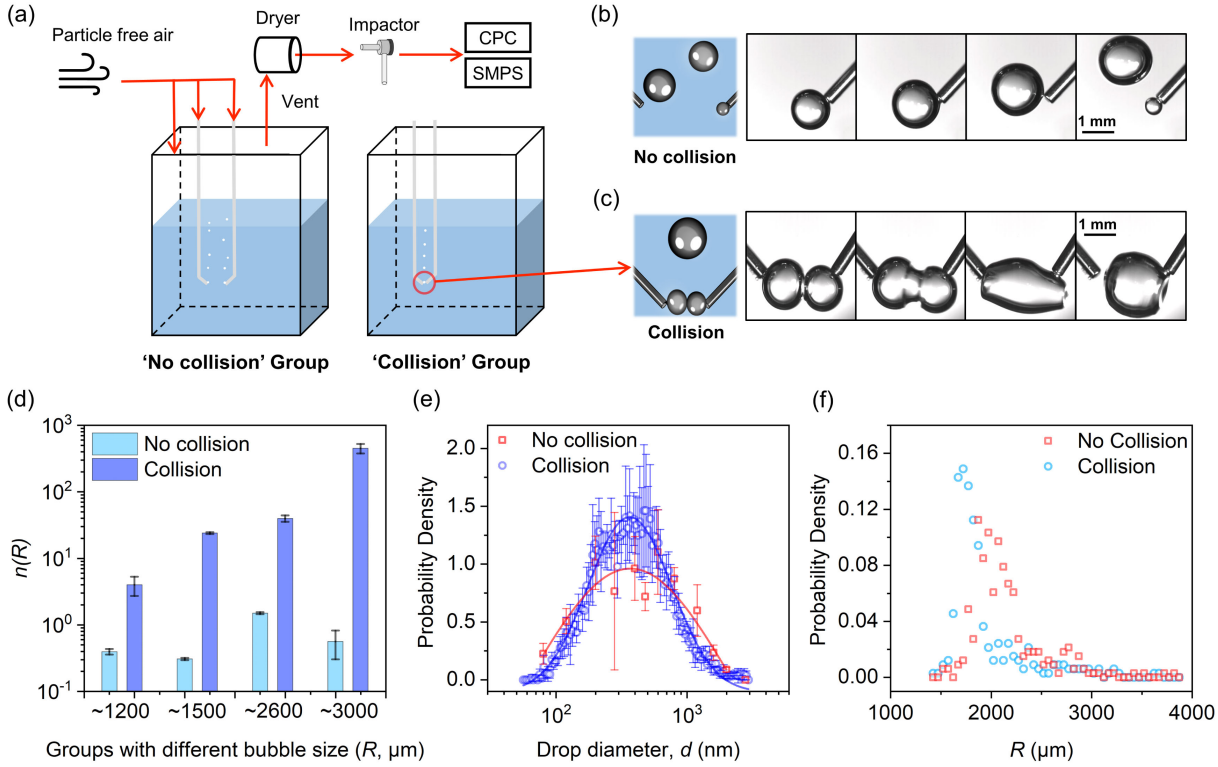

FIG. 2. Assessing the effect of bubble collisions on drop generation. (a) Schematic drawing of the setup for the underwater bubble collision experiment. The distance between the two streams of bubbles decides whether bubbles collide with each other or not. The drop concentrations and size distributions are measured, after removal of the largest drops (impactor) by a condensational particle counter (CPC) and a scanning mobility particle sizer (SMPS). Schematic drawings and snapshots of the bubble formation processes for (b) no collision group (intervals of $6/1000$ s) and (c) collision group (intervals of $1/1000$ s) [21]. (d) Comparison of the number of submicron drops generated per bubble $n(R)$, for different bubble sizes between the no collision and collision groups. (e) Size distributions of drops (d, the drops diameter) produced from the no collision and collision bubbles with $R \sim 3000$ μm. (f) Distribution of R of surface bubbles (measured at bubble bursting) from the no collision and collision groups. Collisions make bubbles detach from the needles before they can grow up to their maximum size, resulting in somewhat smaller individual bubble radii with collision as compared to without.

$r \approx 15$ μm for bubbles with $R \approx 1700$ μm is itself larger than a micron. We estimate its velocity from high-speed video as $v_j \approx 2$ m/s, yielding $\mathrm{We} \approx 1$, far below the splashing condition. Analogous to the burst of surface bubbles, underwater collisions between slightly unequal in size bubbles may also lead to the formation of internal jets. The jet diameter follows approximately the "10% rule" [4,18], that is, $r \approx R/10$, with velocity $v_j \approx \sqrt{\sigma/\rho R}$ (modulo corrections involving the liquid viscosity, see, e.g., [7]), leading to $\mathrm{We} \approx 1/10$, far below, again, the splashing threshold. That option is thus ruled out.

We propose, on hand of an analog experiment, that the drops are the fragmentation products of the film squeezed between colliding, then coalescing bubbles, as depicted in Fig. 3(a). When bubbles collide with a nonzero relative velocity, a liquid layer between the flattened bubbles needs to drain and then puncture for coalescence to occur. The radius of the contact area between bubbles of radius R may vary depending on the strength of the collision, but we use R as a representative value for this radius. We simulate the process using a transparent glass tube of radius R, plugged at the top, partially filled with water, with air at the top as the "upper bubble" [Fig. 3(b)]. After slowly lifting the bottom away from the water surface, a section of air (the "lower bubble") rushes toward the water surface in the tube. After contact, the two bubbles are separated by a film that drains and finally bursts, thus completing coalescence. Interestingly, the burst phenomenology is similar to the one known for soap films or very thin bubble caps [Fig. 3(d)]: the film punctures at its border in the marginal regeneration region, and the opening hole flaps like a flag from a shear instability with the ambient air [39]. This mechanism, distinct from the one involving centripetal acceleration on the curved shape of surface bubbles caps [5], is known to also operate for submillimetric surface bubbles [15].

Flapping thin films fragment in tiny drops, making this observation a serious candidate to explain the formation of submicron aerosols from bubbles collisions. The flapping, or Squire instability onsets within a time $t_s \sim \sqrt{\rho/\rho_a}\sqrt{\lambda h}/v$, with $v \sim \sqrt{2\sigma/\rho h}$ as the Culick receding velocity of a film with thickness h after film puncture, forming undulations of wavelength $\lambda \sim h(\rho/\rho_a)$ with ρ_a the

density of the ambient gas [40]. For this instability to affect the film, t_s should be smaller than the transit time R/v of the film receding edge over the film radius R, a condition implying that

$$h < \frac{\rho_a}{\rho} R. \tag{1}$$

This critical film thickness, which scales as the radius of the contact area between the bubbles, is larger in a heavier gas environment. A film between two bubbles of comparable sizes is typically flat, but it drains for the same reason the curved cap of a bubble at the surface of a pool does: the pressure in a bubble cap with radius of curvature R is $p_0 + 2\sigma/R$ with p_0 the external pressure. A flat film squeezed between two bubbles has pressure p_0, but the pressure at the border of the wetting contact area (the tube radius in our analog experiment) is $p_0 - \sigma/R$. In both cases, the liquid is pressurized with respect to its environment where it empties and thins until it finally ruptures [5,33]. The thinning dynamics (see details in Supplemental Material [21]) leads to $h(t) \sim R(t/t_v)^{-2/3}$, where $t_v \sim \eta R/\sigma$ is a viscous time, and η is the liquid velocity. The bursting time corresponds to the contamination time at the film edge [33] given by $T \sim (h/u)\mathrm{Sc}^{2/3}$ where $\mathrm{Sc} = \nu/D$ (with $\nu = \eta/\rho$ and D is a mass diffusivity) is the Schmidt number of the impurities feeding the marginal regeneration responsible for the film integrity, and drainage dynamics at velocity $u \sim (\sigma/\eta) \times (h/R)^{3/2}$. The bursting condition $T < R/u$ provides the bursting time $t_\star \sim t_v \mathrm{Sc}$, and the film thickness at burst

$$h(t_\star) = R\mathrm{Sc}^{-2/3}. \tag{2}$$

Combining Eqs. (1) and (2), a ruptured film will spontaneously flap provided $\mathrm{Sc}^{2/3}(\rho_a/\rho) > 1$, a condition, with $\mathrm{Sc} = \mathcal{O}(10^6)$ always fulfilled in air [where $\rho_a/\rho = \mathcal{O}(10^{-3})$]. Interestingly, this condition puts no constraint on the colliding bubbles contact area R, meaning that whatever the strength of the collision may be (R is larger for a stronger bubble collision velocity), flapping is likely to occur identically.

The size of the drops d thus produced scales like, but is typically much smaller than R [3],

$$d \sim \sqrt{vt_s h} \sim h\sqrt{\frac{\rho}{\rho_a}} \sim R\mathrm{Sc}^{-2/3}\sqrt{\frac{\rho}{\rho_a}} = \mathcal{O}(R/10^3), \tag{3}$$

predicting that drops produced by millimeter-size colliding bubbles are micronic, consistent with Fig. 2(e). Finally, Eqs. (1) and (3) predict that film flapping should occur faster and produce finer aerosols in denser gases [15]. This prediction aligns with the observations in Fig. 3(e) showing that film flapping has a larger amplitude in an SF_6 environment, resulting in an earlier and more complete film fragmentation compared to air.

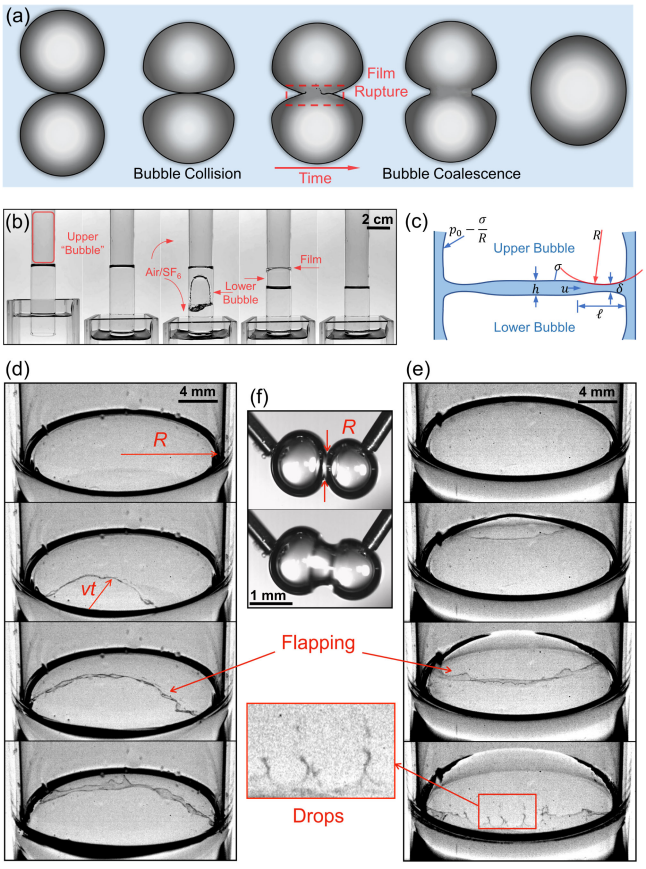

FIG. 3. Film fragmentation and drop production during bubble collision. (a) Schematic illustration of the proposed film fragmentation process during an underwater bubble collision. (b) Analog of a bubble-bubble collision in a glass tube. A liquid film is squeezed between two gas compartments in a glass tube, analogous to the contact area between two colliding bubbles. (c) Schematic diagram of the film and parameters governing its drainage before rupture. A sequence of flapping film at burst during an analog bubble-bubble collision [(d) air-water interface; (e) SF_6-water interface], captured at intervals of 1/2250 s (see videos in Supplemental Material [21]) showing the generation of liquid ligaments and drops. (f) Snapshots before and after the film rupture during a bubble collision event from Fig. 2(c), where R is the radius of the contact area between the two bubbles, namely, the radius of the glass tube in the analog experiment.

In summary, we have shown that bubbles densely packed in space, liable to undergo collisions as those formed at high airflow rate through a needle or pores, produce large numbers of submicron drops. This new insight invites one to reevaluate a number of previous studies [15,41–47] that have employed airflows exceeding critical for bubble generation. Notable examples include those examining the physicochemical properties of nascent sea spray aerosols at airflow rates of 1–9 L/ min [42], laboratory simulations of sea spray aerosols at 5–10 L/ min [43], and investigations of the impact of surfactants on submicron sea spray aerosol production at 50–100 ml/ min [44], as well as our previous work [15] utilizing submerged needles or

sintered filter plates for bubble generation: tests with $R \sim 1000$ μm actually used an airflow exceeding the threshold for collisions. The drops witnessed there are likely to originate from flapping film fragmentation that had occurred during underwater bubble collisions, rather than at surface bursting.

Our results demonstrate that aerosol production is not solely confined to the surface of water, but that it should be sought for in the abyss: underwater bubble collisions contribute significantly more to the formation of submicron drops than was previously recognized. This finding fundamentally shifts our understanding of spray aerosol production and invites us to reconsider the mechanisms from which they originate, notably bubble collisions, in all the relevant environmental and industrial processes where they arise.

We thank Professor Peng Tan for providing a high-speed camera and Professor Yuanlong Huang for assisting with the particle size distribution measurements. This work was supported by the National Natural Science Foundation of China (No. 42377090 and No. 42077193), the Shanghai Natural Science Foundation (23ZR1479700), and the National Key RD Program (No. 2022YFC3702600 and No. 2022YFC3702601).

*Contact author: emmanuel.villermaux@univ-amu.fr
†Contact author: xiaofeiwang@fudan.edu.cn

[1] A. H. Woodcock, C. F. Kientzler, A. B. Arons, and D. C. Blanchard, Giant condensation nuclei from bursting bubbles, Nature (London) **172**, 1144 (1953).
[2] F. Veron, Ocean spray, Annu. Rev. Fluid Mech. **47**, 507 (2015).
[3] E. Villermaux, X. Wang, and L. Deike, Bubbles spray aerosols: Certitudes and mysteries, PNAS Nexus **1**, pgac261 (2022).
[4] E. R. Lewis and S. E. Schwartz, *Sea Salt Aerosol Production: Mechanisms, Methods, Measurements and Models* (American Geophysical Union, Washington, DC, 2004), 10.1029/GM152.
[5] H. Lhuissier and E. Villermaux, Bursting bubble aerosols, J. Fluid Mech. **696**, 5 (2012).
[6] B. Stevens and G. Feingold, Untangling aerosol effects on clouds and precipitation in a buffered system, Nature (London) **461**, 607 (2009).
[7] L. Deike, Mass transfer at the ocean–atmosphere interface: The role of wave breaking, droplets, and bubbles, Annu. Rev. Fluid Mech. **54**, 191 (2021).
[8] K. Sampath, N. Afshar-Mohajer, L. D. Chandrala, W. Heo, J. Gilbert, D. Austin, K. Koehler, and J. Katz, Aerosolization of crude oil-dispersant slicks due to bubble bursting, J. Geophys. Res. **124**, 5555 (2019).
[9] X. Wang, G. B. Deane, K. A. Moore, O. S. Ryder, M. D. Stokes, C. M. Beall, D. B. Collins, M. V. Santander, S. M. Burrows, C. M. Sultana, and K. A. Prather, The role of jet and film drops in controlling the mixing state of submicron sea spray aerosol particles, Proc. Natl. Acad. Sci. U.S.A. **114**, 6978 (2017).
[10] S. D. Brooks and D. C. Thornton, Marine aerosols and clouds, Annu. Rev. Mater. Sci. **10**, 289 (2018).
[11] S. Yang, T. Zhang, Y. Gan, X. Lu, H. Chen, J. Chen, X. Yang, and X. Wang, Constraining microplastic particle emission flux from the ocean, Environ. Sci. Technol. Lett. **9**, 513 (2022).
[12] P. K. Quinn, T. S. Bates, K. S. Schulz, D. J. Coffman, A. A. Frossard, L. M. Russell, W. C. Keene, and D. J. Kieber, Contribution of sea surface carbon pool to organic matter enrichment in sea spray aerosol, Nat. Geosci. **7**, 228 (2014).
[13] L. Dubitsky, O. McRae, and J. C. Bird, Enrichment of scavenged particles in jet drops determined by bubble size and particle position, Phys. Rev. Lett. **130**, 054001 (2023).
[14] D. E. Spiel, On the births of film drops from bubbles bursting on seawater surfaces, J. Geophys. Res. **103**, 24907 (1998).
[15] X. Jiang, L. Rotily, E. Villermaux, and X. Wang, Submicron drops from flapping bursting bubbles, Proc. Natl. Acad. Sci. U.S.A. **119**, e2112924119 (2022).
[16] F. J. Blanco-Rodríguez and J. M. Gordillo, On the sea spray aerosol originated from bubble bursting jets, J. Fluid Mech. **886**, R2 (2020).
[17] A. Berny, S. Popinet, T. Séon, and L. Deike, Statistics of jet drop production, Geophys. Res. Lett. **48** (2021).
[18] C. F. Brasz, C. T. Bartlett, P. L. L. Walls, E. G. Flynn, Y. E. Yu, and J. C. Bird, Minimum size for the top jet drop from a bursting bubble, Phys. Rev. Fluids **3**, 074001 (2018).
[19] C. D. O'Dowd, M. C. Facchini, F. Cavalli, D. Ceburnis, M. Mircea, S. Decesari, S. Fuzzi, Y. J. Yoon, and J.-P. Putaud, Biogenically driven organic contribution to marine aerosol, Nature (London) **431**, 676 (2004).
[20] D. C. Blanchard and L. Syzdek, Mechanism for the water-to-air transfer and concentration of bacteria, Science **170**, 626 (1970).
[21] See Supplemental Material at http://link.aps.org/supplemental/10.1103/PhysRevLett.133.024001 for details regarding the theoretical derivation, experimental details, experimental results, measurement methods, and evidence for the existence of submicron drops inside the bubbles, which includes Refs. [22–30].
[22] Y. Toba, Drop production by bursting of air bubbles on the sea surface (ii) theoretical study on the shape of floating bubbles, J. Oceanogr. Soc. Jpn. **15**, 121 (1959).
[23] D. C. Blanchard and L. D. Syzdek, Production of air bubbles of a specified size, Chem. Eng. Sci. **32**, 1109 (1977).
[24] T. S. Laker and S. M. Ghiaasiaan, Monte-carlo simulation of aerosol transport in rising spherical bubbles with internal circulation, J. Aerosol Sci. **35**, 473 (2004).
[25] Q. Ma, Y. Zhou, H. Gu, Z. Sun, L. Li, and X. Cui, Experimental research on aerosol deposition phenomenon in single-sized rising bubble, Prog. Nucl. Energy **154**, 104456 (2022).
[26] E. O. Knutson and K. T. Whitby, Aerosol classification by electric mobility: Apparatus, theory, and applications, J. Aerosol Sci. **6**, 443 (1975).
[27] M. R. Stolzenburg, A review of transfer theory and characterization of measured performance for differential mobility analyzers, Aerosol Sci. Technol. **52**, 1194 (2018).

[28] M. R. Stolzenburg and P. H. McMurry, Equations governing single and tandem Dma configurations and a new log-normal approximation to the transfer function, Aerosol Sci. Technol. **42**, 421 (2008).
[29] J. Miguet, F. Rouyer, and E. Rio, The life of a surface bubble, Molecules **26**, 1317 (2021).
[30] A. Gros, A. Bussonnière, S. Nath, and I. Cantat, Marginal regeneration in a horizontal film: Instability growth law in the nonlinear regime, Phys. Rev. Fluids **6**, 024004 (2021).
[31] B. Néel and L. Deike, Collective bursting of free-surface bubbles, and the role of surface contamination, J. Fluid Mech. **917**, A46 (2021).
[32] B. Néel, M. A. Erinin, and L. Deike, Role of contamination in optimal droplet production by collective bubble bursting, Geophys. Res. Lett. **49** (2022).
[33] S. Poulain, E. Villermaux, and L. Bourouiba, Ageing and burst of surface bubbles, J. Fluid Mech. **851**, 636 (2018).
[34] R. Bolaños-Jiménez, A. Sevilla, C. Martínez-Bazán, and J. M. Gordillo, Axisymmetric bubble collapse in a quiescent liquid pool. II. Experimental study, Phys. Fluids **20**, 112104 (2008).
[35] J. M. Gordillo, A. Sevilla, J. Rodríguez-Rodríguez, and C. Martínez-Bazán, Axisymmetric bubble pinch-off at high Reynolds numbers, Phys. Rev. Lett. **95**, 194501 (2005).
[36] T. Séon and A. Antkowiak, Large bubble rupture sparks fast liquid jet, Phys. Rev. Lett. **109**, 014501 (2012).
[37] Y. S. Tian, Z. Q. Yang, and S. T. Thoroddsen, Conical focusing: Mechanism for singular jetting from collapsing drop-impact craters, J. Fluid Mech. **958**, R1 (2023).
[38] G. E. Cossali, A. Coghe, and M. Marengo, The impact of a single drop on a wetted solid surface, Exp. Fluids **22**, 463 (1997).
[39] H. Lhuissier and E. Villermaux, Soap films burst like flapping flags, Phys. Rev. Lett. **103**, 054501 (2009).
[40] E. Villermaux, Fragmentation versus cohesion, J. Fluid Mech. **898**, 1 (2020).
[41] M. Masry, S. Rossignol, B. T. Roussel, D. Bourgogne, P.-O. Bussière, B. R'mili, and P. Wong-Wah-Chung, Experimental evidence of plastic particles transfer at the water-air interface through bubble bursting, Environ. Pollut. **280**, 116949 (2021).
[42] W. C. Keene, H. Maring, J. R. Maben, D. J. Kieber, A. A. P. Pszenny, E. E. Dahl, M. A. Izaguirre, A. J. Davis, M. S. Long, X. Zhou, L. Smoydzin, and R. Sander, Chemical and physical characteristics of nascent aerosols produced by bursting bubbles at a model air-sea interface, J. Geophys. Res. **112**, D21202 (2007).
[43] E. Fuentes, H. Coe, D. Green, G. d. Leeuw, and G. McFiggans, Laboratory-generated primary marine aerosol via bubble-bursting and atomization, Atmos. Meas. Tech. **3**, 141 (2010).
[44] K. Sellegri, C. D. O'Dowd, Y. J. Yoon, S. G. Jennings, and G. d. Leeuw, Surfactants and submicron sea spray generation, J. Geophys. Res. **111** (2006).
[45] A. Aliseda and J. C. Lasheras, Preferential concentration and rise velocity reduction of bubbles immersed in a homogeneous and isotropic turbulent flow, Phys. Fluids **23**, 093301 (2011).
[46] R.-F. Shiu, L.-Y. Chen, H.-J. Lee, G.-C. Gong, and C. Lee, New insights into the role of marine plastic-gels in microplastic transfer from water to the atmosphere via bubble bursting, Water Res. **222**, 118856 (2022).
[47] M. Chen, Y. Xing, J. Kong, D. Wang, and Y. Lu, Bubble manipulates the release of viral aerosols in aeration, J. Hazard. Mater. **461**, 132534 (2024).